Observation of light and secondary ion emissions from surfaces irradiated with highly charged ions

Nishida, Naofumi
Sakurai, Makoto
Kato, Daiji
Sakaue, Hiroyuki A.

(Citation)
Journal of Vacuum Science & Technology B,38(4):044006

(Issue Date)
2020-07

(Resource Type)
journal article

(Version)
Version of Record

JVST B
Journal of Vacuum Science & Technology B

Observation of light and secondary ion emissions from surfaces irradiated with highly charged ions

Cite as: J. Vac. Sci. Technol. B **38**, 044006 (2020); https://doi.org/10.1116/6.0000042
Submitted: 29 January 2020 . Accepted: 26 June 2020 . Published Online: 10 July 2020

Naofumi Nishida, Makoto Sakurai, Daiji Kato, and Hiroyuki A. Sakaue

JVST B
Journal of Vacuum Science & Technology B

ARTICLE

avs.scitation.org/journal/jvb

Observation of light and secondary ion emissions from surfaces irradiated with highly charged ions

Cite as: J. Vac. Sci. Technol. B 38, 044006 (2020); doi: 10.1116/6.0000042
Submitted: 29 January 2020 · Accepted: 26 June 2020 ·
Published Online: 10 July 2020

Naofumi Nishida,[1] Makoto Sakurai,[1,a)] Daiji Kato,[2] and Hiroyuki A. Sakaue[2]

AFFILIATIONS

[1]Department of Physics, Kobe University, 1-1 Rokkodai, Nada-ku, Kobe 657-8501, Japan
[2]National Institute for Fusion Science, 332-6 Oroshi-cho, Toki 509-5292, Japan

Note: This paper is part of the 2020 Special Topic Collection on Secondary Ion Mass Spectrometry, SIMS.
[a)]**Electronic mail:** msakurai@kobe-u.ac.jp

ABSTRACT

Visible light and secondary ions emitted from various sample surfaces (Si, HOPG, Cu, and Teflon) were observed after irradiation with highly charged ions (HCIs). HCIs were produced using an electron beam ion source (Kobe EBIS) at Kobe University. Visible emissions were detected using a liquid nitrogen cooled CCD detector. The mass spectrum of secondary ions was obtained using a quadrupole mass analyzer. The major constituent in both light and secondary ion emissions was hydrogen. Balmer lines were the dominant form of light emission as observed from spectra, and proton signals were the most intense peaks in SIMS spectra. The emission intensity of Balmer light and the proton signal intensity (as observed from the SIMS spectrum) both increased as the charge state of the incident HCI increased. Both intensities were roughly proportional to the third to fourth power of the charge state. Spatial distribution of Balmer light was measured and the kinetic energy of hydrogen sputtered from the surface was estimated to be ~20 eV. The SIMS measurement results for the Teflon sample demonstrate the advantage of using SIMS with an HCI probe for detecting electronegative elements.

I. INTRODUCTION

A highly charged ion (HCI) has a large amount of potential energy, with the specific amount depending on its charge state. The potential energy of an HCI E_p, which is the sum of the binding energies for each ionization step, is approximately proportional to the 2.8th power of its charge state q, that is, $E_p \propto q^{2.8}$. The interaction between an HCI and a surface results in the emission of photons (in the range of visible light to x rays), emission of hundreds of secondary electrons, sputtering of secondary ions, and modification of the surface structure at the nanometer scale.[1–5] These changes are caused by potential energy deposition on the surface. The effects of HCI on surfaces are different from those of singly charged ions (SCIs), as SCIs deposit only their kinetic energy.

We have developed an electron beam ion source at Kobe University (called Kobe EBIS) to produce HCIs and have performed various studies on the interaction of HCIs with surfaces.[6–12] The fluence of incident HCIs used in these experiments was in the range of 10^{12}–10^{14} ions/cm^2. We have previously reported on the emission of Balmer lines that are induced by the irradiation of a surface with HCIs.[13–15] Several types of photons are emitted when surfaces are irradiated with HCIs. For very high charge states, x rays are emitted from incident HCIs, as part of a de-excitation process of a hollow atom created near the surface.[2] In our previous studies, visible light was observed for the spectral range of 420–670 nm. From the spectral and spatial distribution of emitted light, Balmer lines emitted from the space near the surface were dominant. Balmer lines have been observed by other research groups, where a Balmer line (H_α) from a hydrogen adsorbed silicon (Si) surface increased with the charge state of an incident HCI.[16] Several research groups have measured secondary ions stimulated by the injection of HCI, showing that protons are among the dominant ions emitted and their yield rapidly increases with increases in the charge state of incident HCIs.[4,17,18]

In this study, we observed Balmer lines and secondary ions emitted from the vicinity of a surface irradiated with an HCI. These observations were used to study the mechanism by which protons are produced and hydrogen atoms are excited in response to potential energy deposition by HCI.

II. EXPERIMENTAL METHODS

The Kobe EBIS consists of an electron gun, drift tubes, an electron collector, and a superconducting magnet.[6,7] The magnet includes Helmholz coils in order to expand the flat region of magnetic field strength to increase the volume of the trap region. HCIs are created by a successive ionization process that occurs during collision of electrons focused by a strong magnetic field (3 T) with ions. The potential of drift tubes (the acceleration voltage to HCIs) was 3 kV. The pressure of the Kobe EBIS was in the range of 10^{-8} Pa during operation. The HCIs extracted from the Kobe EBIS were in various charge states. The charge states (q) and kinetic energies of Ar HCIs used in the present experiment were in the range of 6–16 and $3q$ keV, respectively. HCIs in a specific charge state were selected using a sector magnet, and they were then transferred into an irradiation chamber that was maintained in ultrahigh vacuum at 10^{-7}–10^{-8} Pa. Primary ion current was monitored using a Faraday cup, and the ion beam shape and position were monitored with a microchannel plate (MCP) detector. Incident ion current to the sample was monitored during irradiation using a homemade electrometer operating on floating potential (max. 2 kV). The sample was mounted on an electrically isolated sample stage with five-axis movement.

The light emissions caused by the interaction between HCIs and samples were measured with a liquid nitrogen cooled charge coupled device (CCD, Roper LN/CCD 1340/1300-E/1). The diameter of the HCI beam was ~3 mm and the beam current of HCI (Ar^{q+}, $q = 6$–16) was in the range of 0.1–1 nA. Spectroscopic measurements were conducted using a homemade polychromator with a commercial flat-field grating (Richardson Gratings, 52066BK-002C). The grating has 813.5 grooves/mm and imaging range of 380–705 nm. The wavelength resolution of the polychromator in the present experimental condition was ~5 nm. Wavelength distribution for the range of 420–670 nm and spatial distribution in the horizontal direction were measured from the two-dimensional CCD image. For spectroscopic measurements, the exposure time was 2 h. For the Balmer line measurement, the distribution of light emission in two-dimensional space was determined using an H_α filter (center wavelength 656 nm, bandwidth ±5 nm, 90% transmittance) instead of a polychromator. The intensity of emission passing through the filter was evaluated and the exposure time was 10 min.

Secondary ion mass spectrometry (SIMS) was performed using a quadrupole mass analyzer (QMS, ULVAC MSQ-200) installed in the irradiation chamber, as shown in Fig. 1. In the QMS, ions are detected by an electron multiplier. For SIMS measurement, the sample surface was tilted 45° against the incident HCI beam, while light emission was observed under normal incidence conditions. An electrostatic lens was mounted in front of the QMS instead of an ion source.

Si, highly oriented pyrolytic graphite (HOPG, SPI Supplies), copper (Cu, polycrystalline OFHC plate, 99.96% purity), and Teflon plates were used as samples. We used commercially available, mirror polished Si wafers for Si samples. No cleaning treatments were performed in vacuum for the Si samples. For the HOPG sample, the topmost surface layers were peeled off with adhesive tape before transferring into vacuum. Because no cleaning or passivation procedures were conducted for Si samples, native oxide films were formed on the surfaces. Each sample was mounted on a sample holder and transferred to the irradiation chamber using a two-step load-lock system and irradiated with HCIs.

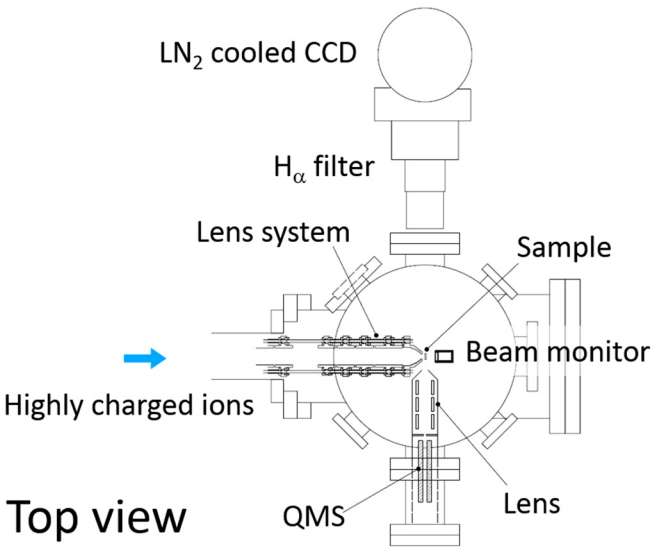

FIG. 1. Schematic drawing of the irradiation chamber.

III. RESULTS AND DISCUSSION

A. Balmer line emission

The visible emission spectrum from the Cu sample irradiated with Ar^{11+} ions is shown in Fig. 2. Balmer lines (H_α at 656 nm and H_β at 486 nm), an Na D line at 589 nm, and Cu I lines at 510–520 nm are observable. Among these lines, H_α has the highest intensity. Balmer lines were observed for all samples. For the

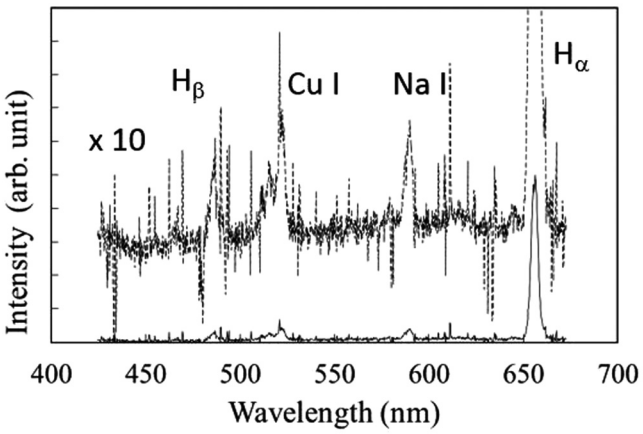

FIG. 2. Visible emission spectrum from Cu irradiated with Ar^{11+}.

HOPG sample, only Balmer lines were observed. The sodium signal was attributed to contamination on the sample.

Our previous research showed that the intensity of Balmer lines increases with increasing charge state of the incident HCI and that it did not depend on the kinetic energy of the HCI.[13,14] This means Balmer line emission is exclusively caused by potential energy deposition from the HCI. Our previous experiment on how irradiation time affects Balmer line intensity emitted from the HOPG surface indicated that emission intensity decreased with increasing irradiation time. This result suggests that a hydrogen atom in a water molecule adsorbed on the surface desorbs in an excited state (with certainty) as a consequence of the HCI/surface interaction.[15] The detailed mechanism for the production of excited hydrogen atoms stimulated by the HCI's deposition of potential energy on the surface still remains unclear.

In order to determine the kinetic energy of the excited hydrogen atom released from the HCI-irradiated surface, we measured the spatial distribution of the Balmer line. The excited hydrogen atom is created at the sample surface and leaves the surface, emitting a Balmer line during its flight, so the light intensity decays exponentially with the distance from the surface, provided the kinetic energy of excited hydrogen atom has a similar value. Figure 3 shows the intensity distribution of Balmer line (H_α) as a function of distance from the HOPG surface irradiated with Ar^{q+} ($q = 6, 8, 11, 14, 16$). The position at 0 mm on the horizontal axis indicates that of the sample surface. Judging from the spread of rising at 0 mm, the spatial resolution is estimated at ~0.5 mm. Excited hydrogen is released in various directions, so the measured distribution may not accurately express the density distribution normal to the surface. However, we roughly estimated the kinetic energy by fitting an exponential curve to the distribution from Fig. 3. The curves in Fig. 3 do not show obvious charge state dependence, that is, each curve decays with a similar attenuation coefficient. Assuming that the reciprocal of Einstein's A coefficient of hydrogen atom $A_{32} = 0.96 \times 10^8$/s at the electron transition from quantum number 3 to 2 corresponds to the lifetime of the excited level, the kinetic energy of the excited hydrogen released from the surface was estimated to be ~20 eV on average with the uncertainty of ~5 eV. This value is much higher than what has been reported for secondary ions produced by HCI's impact.[19] There may be an acceleration mechanism in effect for the secondary ion, which captures an electron to the excited state of the ion.

B. SIMS measurement

The SIMS spectrum of the Si sample irradiated with Ar^{q+} ($q = 6, 16$) is shown in Fig. 4. Hydrogen, sodium, and silicon peaks are visible in the spectrum. Hydrogen and sodium elements were observed in the corresponding emission spectrum from a previous study.[15] The SIMS spectrum shows that silicon ions were emitted from the sample surface; however, no excited silicon atoms were observed near the surface. The proton signal increased as the charge state of incident HCI increased, while signals of other elements did not change significantly.

Figure 5 shows the charge state dependence of atomic ion peak intensities for H, Na, and Si observed in the SIMS spectrum of an Si sample irradiated with Ar^{q+}. The proton intensity increases nonlinearly, while other elements did not exhibit dependence on charge state. This charge state dependence of the proton signal shows similar tendency to that of Balmer light emission where the emission intensity increases at a rate of third to fourth power of the charge state.[12] These results suggest that a similar desorption mechanism is responsible for proton emission and hydrogen atom excitation.

Charge state dependence (or potential energy dependence) of proton yield has been studied previously on hydrogen-terminated silicon surfaces (Si–H) and native oxide covered silicon surfaces (SiO_2/Si), where secondary ions were analyzed by using the time of flight (TOF) technique.[4,17,18] The potential energy (E_p) dependence of proton yield (Y) has been reported to be $Y \propto E_p^{0.6}$ for SiO_2/Si surfaces and $Y \propto E_p^{1.1}$ for the Si–H surface.[4] These values roughly correspond to charge state dependences of $Y \propto q^{1.7}$ for SiO_2/Si and $Y \propto q^{3.1}$ for Si–H. The Si sample used in the present study consisted

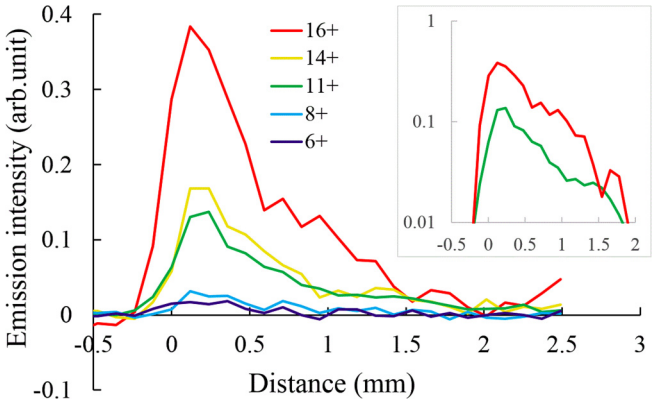

FIG. 3. Spatial distribution of Balmer line (H_α) intensity from an Si surface irradiated with Ar^{q+}. Semilogarithmic plots for Ar^{11+} and Ar^{16+} are shown in the inset.

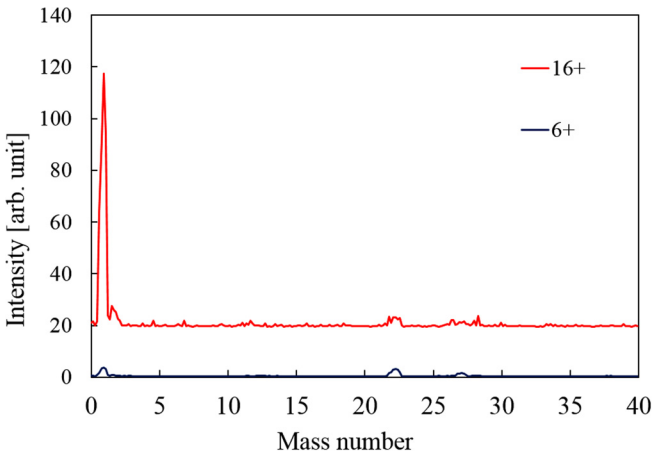

FIG. 4. SIMS spectrum of Si irradiated with Ar^{q+} ($q = 6, 16$).

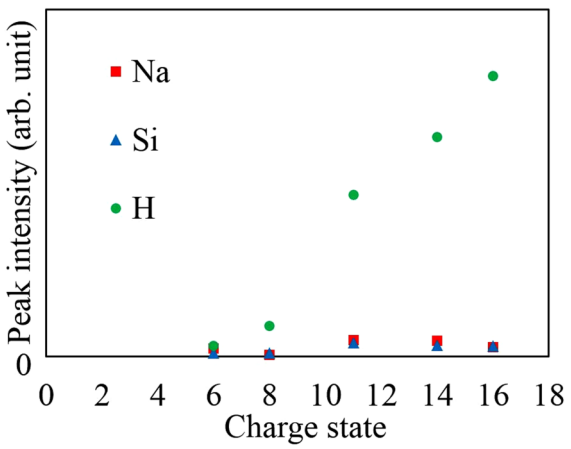

FIG. 5. Charge state dependence of H, Na, and Si peak intensities observed in SIMS spectrum of Si irradiated with Ar^{q+}.

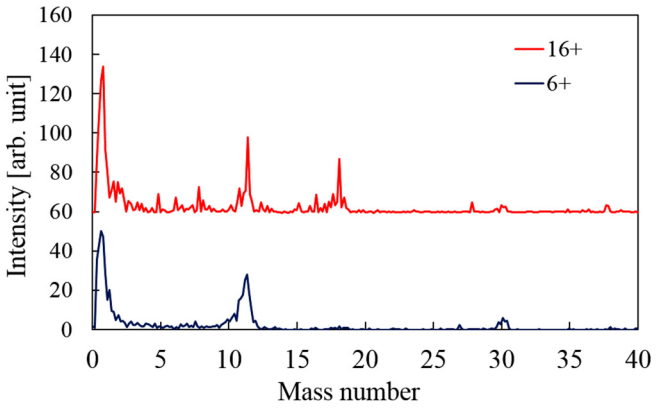

FIG. 6. SIMS spectrum of Teflon plate irradiated with Ar^{q+} ($q = 6, 16$).

of an SiO_2/Si structure. However, our charge state dependence results showed a greater resemblance to those for the Si–H system. These differences may be attributed to a difference in measurement methods. Previous experiments used the TOF technique while we used a QMS. The TOF technique used in the previous experiments has unique features such that the start signal for flight time measurement using a multistop time-to-digital convertor is provided with secondary electron signal and that the transmission efficiency is high.[18] On the other hand, the TOF technique has limitations: the incident ion intensity is limited less than 10^4 cps to avoid accidental coincidence and the possibility of counting inaccuracy, that is, multiple ion emissions induced by a single HCI incidence cannot be recognized, because two or more ions enter the detector simultaneously and are recorded as a single count. The evidence of multiple emission in the TOF measurement has been reported using the pulse height distribution of the MCP signal.[4,20] In contrast, in QMS, the chance of two or more ions with the same m/q value arriving at the detector at the same time is rare because the transmission efficiency of QMS is low. Thus, when the incident HCI intensity is as high as the present experimental condition (10^7–10^9 cps), QMS is thought to be suitable to obtain precise data on the charge state dependence of secondary ion yields.

The SIMS spectrum of the Teflon plate irradiated with Ar^{q+} ($q = 6, 16$) is shown in Fig. 6. The fluorine (F) signal is intense in addition to that of hydrogen and carbon in the spectrum of Ar^{16+}, while in the spectrum of Ar^{6+}, the F signal is negligibly small. The existence of positive F ions is characteristic of SIMS results when probing with HCI. This is because the detection efficiency of electronegative elements is typically low for SIMS, which uses a singly charged Ar beam probe. This advantage of HCI-probed SIMS in the detection of electronegative elements has been demonstrated previously.[20,21] In the secondary ion yield from TiO_2 irradiated with HCI, the oxygen ion signal was negligible for lower charge states and the yield increased rapidly with increases in the charge state, while titanium ion was detected even at low charge states. In contrast, the secondary ion yield for the sputtering by singly charged ions varies over several orders of magnitude with the target element.[22] This means that SIMS with an HCI probe is superior for detecting electronegative elements over ordinary SIMS.

IV. SUMMARY AND CONCLUSIONS

Visible light emission and secondary ion emission were measured for various sample surfaces irradiated with HCIs. The major constituent in both light emission and secondary ion emission was hydrogen. Balmer lines were the dominant form of light emission as observed from spectra, and proton signals were most intense in the SIMS spectra. The intensities of Balmer light emission and proton signals increased in the SIMS spectrum as the charge state of incident HCI increased. The intensities were roughly proportional to the third to fourth power of the charge state for both. Spatial distribution of Balmer light was measured, and the kinetic energy of hydrogen sputtered from the surface was estimated to be ~20 eV. This value is much higher than what has been reported for secondary ions produced by HCI impact. The results from SIMS measurement of the Teflon sample demonstrate the advantage of SIMS using an HCI probe for the detection of electronegative elements. The phenomena of hydrogen and proton emission from surfaces stimulated by HCI injection provide interesting questions that can be the focus of future research. Using SIMS measurement in conjunction with observation of Balmer light emission can provide a useful basis for addressing these questions.

REFERENCES

[1]F. Aumayr, H. Kurz, D. Schneider, M. A. Brieere, J. W. McDonald, C. E. Cunningham, and H. P. Winter, Phys. Rev. Lett. **71**, 1943 (1993).
[2]F. Aumayr and H. P. Winter, Nucl. Instrum. Methods Phys. Res. Sect. B **233**, 111 (2005).
[3]H. Watanabe, S. Takahashi, M. Tona, N. Yoshiyasu, H. Nakamura, M. Sakurai, C. Yamada, and S. Ohtani, Phys. Rev. A **74**, 042901 (2006).
[4]M. Tona, S. Takahashi, K. Nagata, N. Yoshiyasu, C. Yamada, H. Nakamura, S. Ohtani, and M. Sakurai, Appl. Phys. Lett. **87**, 224102 (2005).
[5]M. Tona *et al.*, Surf. Sci. **601**, 723 (2007).

[6]M. Sakurai, H. A. Sakaue, H. Watanabe, N. Nakamura, S. Ohtani, Y. Kawase, K. Mitsumori, T. Terui, and S. Mashiko, Shinku **50**, 390 (2007) (in Japanese).
[7]M. Sakurai *et al.*, Vacuum **84**, 530 (2010).
[8]S. Liu *et al.*, J. Surf. Sci. Nanotechnol. **9**, 241 (2011).
[9]M. Sakurai, S. Liu, S. Sakai, S. Ohtani, T. Terui, and H. A. Sakaue, Nucl. Instrum. Methods Phys. Res. Sect. B **315**, 248 (2013).
[10]N. Nishida, K. Betsumiya, M. Sakurai, T. Sakurai, T. Terui, and S. Honda, J. Surf. Sci. Nanotechnol. **16**, 356 (2018).
[11]N. Nishida, Y. Hori, M. Sakurai, Y. Hujiwara, S. Honda, M. Terasawa, T. Yamaguchi, K. Ishibashi, and H. Izumi, Jpn. J. Appl. Phys. **58**, SIIC01 (2019).
[12]N. Nishida *et al.*, X-Ray Spectrom. **49**, 99 (2020).
[13]M. Sakurai, T. Miyamoto, K. Sasaki, D. Kato, and H. A. Sakaue, J. Vac. Soc. Jpn. **58**, 147 (2015) (in Japanese).
[14]M. Sakurai, K. Sasaki, T. Miyamoto, D. Kato, and H. A. Sakaue, J. Surf. Sci. Nanotechnol. **14**, 1 (2016).
[15]N. Nishida, Y. Hori, A. Yamauchi, M. Sakurai, D. Kato, and H. A. Sakaue, J. Phys. Conf. Ser. **1220**, 012037 (2019).
[16]J. Deiwiks, G. Schiwietz, S. R. Bhattacharyya, G. Xiao, and R. Hippler, Nucl. Instrum. Methods Phys. Res. Sect. B **248**, 253 (2006).
[17]K. Kuroki, K. Komaki, and Y. Yamazaki, Nucl. Instrum. Methods Phys. Res. Sect. B **203**, 183 (2003).
[18]M. Tona, K. Nagata, S. Takahashi, N. Nakamura, N. Yoshiyasu, M. Sakurai, C. Yamada, and S. Ohtani, Surf. Sci. **600**, 124 (2006).
[19]N. Okabayashi, K. Komaki, and Y. Yamazaki, Nucl. Instrum. Methods Phys. Res. Sect. B **235**, 438 (2005).
[20]M. Tona, H. Watanabe, S. Takahashi, N. Nakamura, N. Yoshiyasu, M. Sakurai, C. Yamada, and S. Ohtani, Nucl. Instrum. Methods Phys. Res. Sect. B **258**, 163 (2007).
[21]M. Tona, Y. Fujita, C. Yamada, and S. Ohtani, Phys. Rev. B **77**, 155427 (2008).
[22]H. A. Storms, K. F. Brown, and J. D. Stein, Anal. Chem. **49**, 2023 (1977).